JOURNAL OF SPACECRAFT AND ROCKETS
Vol. 34, No. 3, May–June 1997

Pressure Distribution on Sabots in Hypervelocity Flight

Martin J. Guillot,* Jason N. Dick,* and William G. Reinecke†
University of Texas at Austin, Austin, Texas 78759

Experimental and computational investigations of the pressure distribution on sabots in hypervelocity flight are performed to investigate the accuracy of a computational model previously developed for predicting sabot discard trajectories. The pressure distribution on the sabot front scoop and underside are measured experimentally and compared to results predicted by the modified numerical code. The results of this study indicate that although, overall, the modified code does a reasonable job of predicting sabot trajectories, further refinement to the pressure modeling in the code may be needed. Specifically, refinement to the sabot front scoop pressure model is indicated. Additionally, a simple analytical model developed to help verify the trends predicted by the code is shown to produce accurate results, especially considering the simplicity of the model.

Nomenclature

A_s = total surface area on sabot side faces
$F_{\bar{y}f}$ = net force acting on front scoop in $\bar{y}$ direction for analytical model
$I_{\bar{x}}$ = axial moment of inertia of sabot about tail for analytical model
l_i = axial length of sabot at inner radius
M_t = net moment about tail of sabot
P_o = stagnation pressure behind normal shock corresponding to freestream conditions
P_2 = pressure on underside of sabot corresponding to Prandtl–Meyer expansion from sonic conditions around front scoop to sabot underside
r_i, r_o = inner and outer sabot radii, respectively
S_b = beginning of pressure pulse on sabot underside
S_e = end of pressure pulse on sabot underside
V = freestream velocity
x, y = Cartesian coordinates in unrotated (projectile) coordinates
$\bar{x}, \bar{y}$ = Cartesian coordinates in rotated (sabot) coordinates
α = sabot angle of attack
θ_f = angle of sabot front scoop
ϕ_o = half-angle of sabot petal in circumferential direction

Introduction

THE U.S. Army is interested in developing kinetic energy penetrators with launch velocities on the order of 2.0–2.5 km/s. These projectiles are normally sabot launched. A sabot is a device usually made of two or more petals that encases the projectile, providing needed structural support during launch. Because most projectiles are subcaliber, i.e., projectile diameter smaller than the barrel diameter, the sabot fills the space between the projectile and barrel wall, preventing the muzzle gases from blowing by the projectile. However, after the launch package has exited the muzzle, the sabot becomes parasitic mass and must be removed as quickly as possible to allow low-drag flight of the projectile to the target. This is normally accomplished by incorporating a scoop into the front of the sabot so that aerodynamic forces lift and rotate each petal away from the projectile. A sketch of a simple sabot is shown in Fig. 1.

Sabot separation is a highly complex, unsteady, aerodynamic process. It is essential to understand sabot separation dynamics to ensure that the sabot separates quickly and without inducing perturbing forces that could adversely affect the trajectory of the penetrator. An accurate knowledge of the aerodynamic forces acting on the sabot is essential to predict the dynamic behavior during the discard process. In turn, this requires an accurate knowledge of the pressure distribution on the sabot at all points in the trajectory.

To address this issue, an experimental investigation into the pressure distribution over sabots was initiated. The pressure distribution was measured on the front scoop and underside of one petal of a four-petal sabot at four angles of attack (AOA): 3, 7, 14, and 23 deg. Splitter plates were used to simulate the planes of symmetry created by the presence of the other sabot petals. The experimental results were compared to a numerical model to assess the accuracy of the aerodynamic model used for computing the pressure distribution on the sabot. The experimental investigation was performed in the Mach 5 wind tunnel at the University of Texas at Austin.

Pressure Modeling

Theoretically, one could compute the pressure distribution on the sabot using the full Navier–Stokes equations and couple this solution to the dynamic equations governing the motions of the sabot petals to compute sabot trajectories accurately. In the past, such intensive computations were not feasible. With increasing computational power, it is now possible to solve the fully coupled problem of bodies in relative motion in a flowfield. These investigations provide needed insight into the important physics dominating the sabot separation process. However, computation of the fully coupled problem is still too expensive and time-consuming to be used as a practical design tool.

Customarily, aerodynamic forces acting on the sabot petals are approximated using simpler aerodynamic models. The computer implementation of one model[1–6] was obtained by the Institute for Advanced Technology (IAT) to use in conjunction with its hypervelocity utility research program to compute sabot trajectories of launch packages launched at the IAT Hypervelocity Launch Facility. The code, known as the AVCO code, was originally written to compute the trajectories of sabots made of the simple geometry shown in Fig. 1. However, sabots of current interest are significantly more complex. Two typical launch packages currently used by the IAT are shown in Fig. 2. Both sabots have a nonconstant outer radius, and the sabot in Fig. 2b has a forward ramp on the front scoop. These geometric features, as well as the resulting changes in the aerodynamics, are not modeled in the original AVCO code.

The original geometry and aerodynamic model in the code were found to be inadequate for computing the sabot trajectories of current interest. In an effort to improve and update the code, the geometry and aerodynamic modeling in the original code were modified[7,8] to compute sabot trajectories of the sabots shown in Fig. 2.

Although the modifications improved the radial and angular displacement predictions, the code still tends to overpredict the radial displacement. Sample results for the sabot shown in Figs. 2a and 2b are presented in Figs. 3 and 4, respectively. In Fig. 3, the results from the original version of the AVCO code also are shown. However, in Fig. 4, only the results from the modified version of the

Received Oct. 7, 1996; revision received Dec. 2, 1996; accepted for publication March 12, 1997.

*Research Engineer, Institute for Advanced Technology. Member AIAA.
†Technical Director, Institute for Advanced Technology. Associate Fellow AIAA.

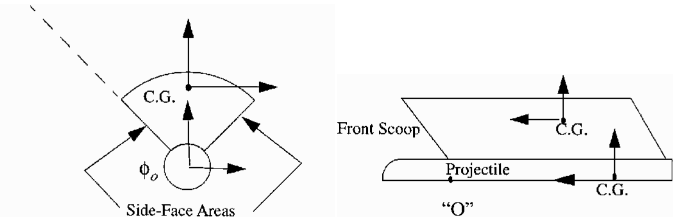

Front view Side view

Fig. 1 Original sabot geometry.

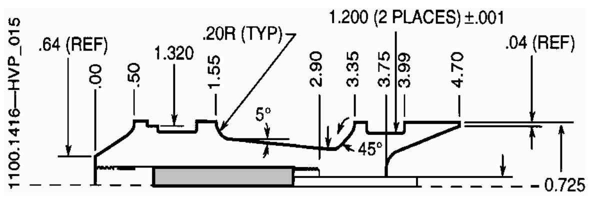

a)

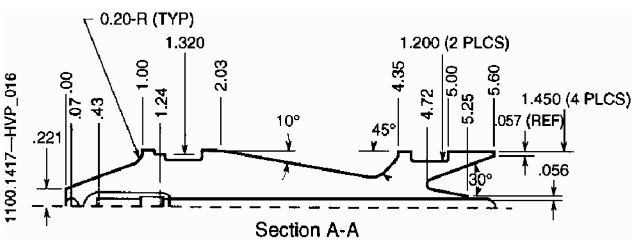

b)

Fig. 2 Typical IAT laboratory sabot penetrator launch packages. Note: dimensions are in inches.

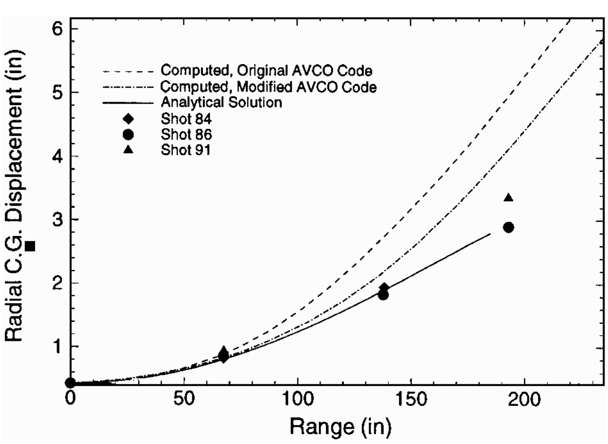

Radial displacement

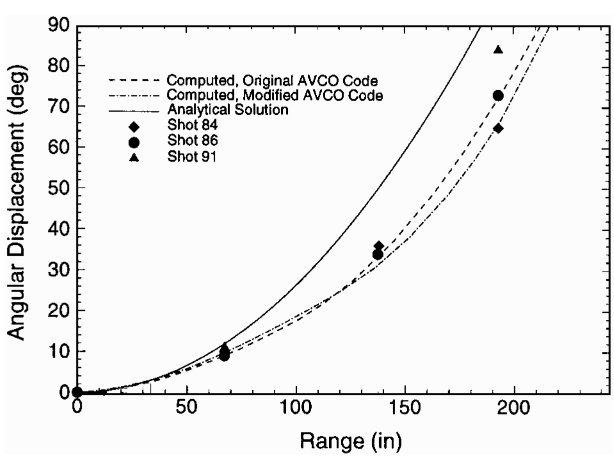

Angular displacement

Fig. 3 Radial and angular displacement HVP_015 sabot (pressure = 430 torr).

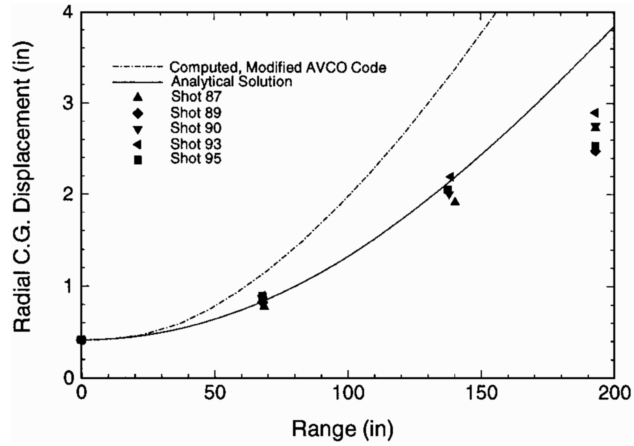

Radial displacement

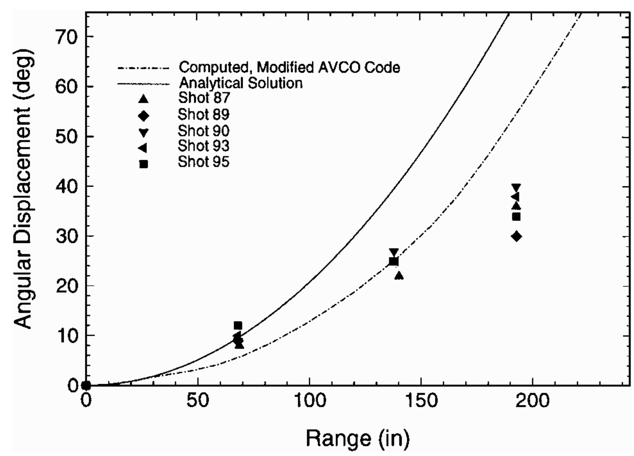

Angular displacement

Fig. 4 Radial and angular displacement HVP_016 sabot (pressure = 500 torr).

code are shown because it is not possible to model the forward ramp on the front scoop with the original version of the code. Figures 3 and 4 show radial and angular displacement of one sabot petal of a four-petal sabot as a function of range. In both cases, the freestream Mach number is 7.5, and the freestream pressures are given in the captions. The experimental data are deduced from flash x-ray photography for the data points at $x = 64$ and 139 in. and from witness plate data at $x = 193$ in. The results show that the AVCO code predicts the angular displacement fairly well but overpredicts the radial displacement. Figures 3 and 4 also show predictions of a simple analytical model.[7] It is seen that the analytical model predicts the radial displacement well but overpredicts the angular displacement.

The overprediction of the radial and angular displacements most likely results from inadequate pressure modeling in the code, specifically, the pressure modeling on the sabot front scoop and underside. The AVCO code incorporates a pressure model based on two-dimensional inviscid gasdynamics applied to the centerline of the sabot. On the front scoop, the code assumes that the pressure is uniformly at stagnation pressure behind a normal shock corresponding to the freestream Mach number. On the underside, the code predicts the base pressure, assuming the flow undergoes a Prandtl–Meyer expansion around the corner of the front scoop. In addition to the base pressure, the code adds a pressure pulse based on experimental data[9] that show a pressure increase in the axial direction from tip to tail due to shock interactions and reflections, and a pressure increase at the tail of the sabot due to flow choking. The empirical procedure for locating the pressure pulse on the sabot underside is sketched in Fig. 5. Briefly, the beginning of the pressure pulse is determined by projecting the line formed by the front scoop to the point where it intersects the projectile, and then projecting it back up to the sabot at a right angle to the sabot underside. The end of the pressure pulse is determined by reflecting a Mach wave from the same location

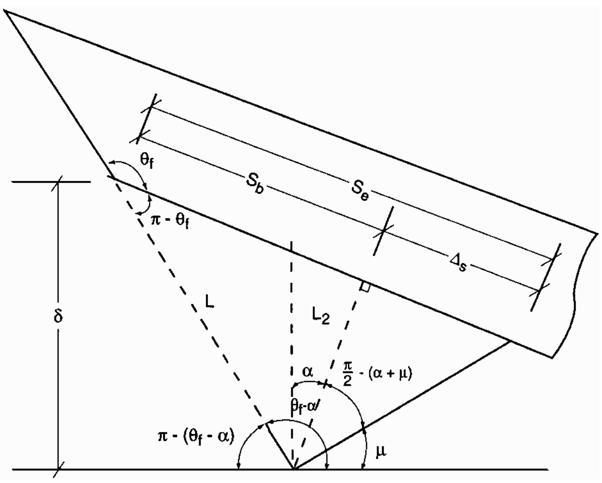

Fig. 5 Empirical procedure to determine location of pressure pulse on sabot underside.

on the projectile back up to the point where it intersects the underside of the sabot. The pressure pulse is assumed to be triangular with the maximum value, based on experimental data, occurring halfway between S_b and S_e. The magnitude of the pressure increase at the tail of the sabot is predicted on the basis of a throttling model. These procedures were developed by Crimi and Siegelman.[1,2] The authors conclude, on the basis of comparison to experimental data, that the empirical model is an accurate representation of the pressure increase along the underside of the sabot.

The empirical procedure to model the underside pressure was developed for sabots with simple conical front scoops and based on experimental data using like sabots. However, the effect a forward ramp has on the flowfield on the underside of the sabot is unknown. If the effect of the forward ramp is to diminish the pressure pulse on the underside of the sabot, then this offers a possible explanation for why the code predicts the angular displacement accurately but overpredicts the radial displacement. For much of the trajectory, the pressure pulse predicted by the code is nearly centered about the sabot center of gravity, so that the moments produced by the pulse tend to cancel. However, the pulse still produces a net lifting force.

Analytical Model

To help verify the trends predicted by the AVCO code, a simple analytical model was developed and the results compared to the code. A schematic of the analytical model is shown in Fig. 6. The model assumes that the pressure on the front scoop is the stagnation pressure behind a normal shock at the freestream Mach number and that the flow at the corner point where the front scoop intersects the underside of the sabot is at sonic conditions corresponding to an isentropic expansion from conditions behind the normal shock. The flow then turns through a Prandtl–Meyer expansion around the corner. Because conditions just before the corner are assumed sonic, the Prandtl–Meyer function on the underside is simply $\nu(M_2) = \pi - \theta_f$. Knowing the value of ν, we can determine the Mach number after the Prandtl–Meyer expansion.

With these pressures acting on the front scoop and underside of the sabot, the forces and moments acting on the sabot petal are summed assuming that the sabot pivots about the aft end. Summing moments about the sabot tail and integrating twice with respect to time yields the AOA as a function of time. The expression for M_t is written as

$$M_t = \left[\frac{P_o \sin\phi_o}{\sin^2\theta_f}\left(\frac{r_o^3 - r_i^3}{3}\right) + (r_i \cot\theta_f + l_i)F_{\bar{y}f} + P_2 \sin\phi_o A_s l_i\right] \tag{1}$$

The entire right-hand side expression is constant for a given geometry and freestream condition, and so, the equation can easily be integrated twice to obtain an expression for the angular velocity and displacement of the sabot petal. The resulting equation is converted to a function of downrange position by introducing the projectile velocity into the equation, i.e., $t = x/V$. The resulting equation is simply

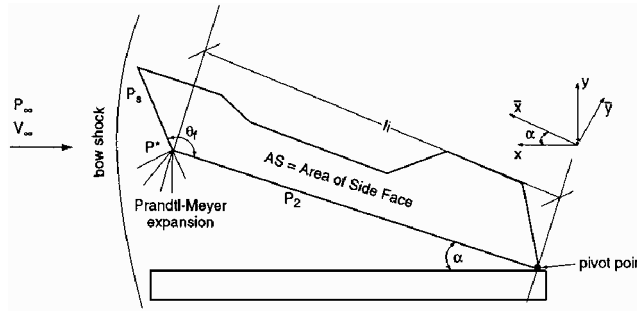

Fig. 6 Analytical model.

$$\alpha(x) = \frac{M_t x^2}{2I_{\bar{x}}V^2} \tag{2}$$

Next, the forces in the y direction are summed to obtain an expression for the radial displacement as a function of downrange position x. Summing forces and integrating yields

$$\begin{aligned} r(x) = {} & \frac{2\sin\phi}{mV^2}\left[(r_i l_i + A_s)P_2 - P_o\left(\frac{r_o^2 - r_i^2}{2}\right)\cot\theta_f\right] \\ & \times\left[\sum_{n=0}^{\infty}\frac{(-1)^n}{(2n)!}\left(\frac{M_t x^2}{2I_{\bar{x}}V^2}\right)^{2n}\frac{x^2}{(4n+1)(4n+2)}\right] \\ & - 2P_o\phi_o\left(\frac{r_o^2 - r_i^2}{2}\right) \\ & \times\left[\sum_{n=0}^{\infty}\frac{(-1)^n}{(2n+1)!}\left(\frac{M_t x^2}{2I_{\bar{x}}V^2}\right)^{2n+1}\frac{x^2}{(4n+3)(4n+4)}\right] \end{aligned} \tag{3}$$

Although the solution is given as an infinite series, experience has shown that the series converges very quickly. For the results presented in this work, the series expansion converged within three terms.

Computational and Experimental Investigation

The experiments were performed in the Mach 5 Wind Tunnel at the University of Texas at Austin.[10] The experimental conditions were $M_\infty = 4.95$, $P_\infty = 0.6715$ psi, and $V_\infty = 2734$ ft/s.

Before discussing the experimental results, several issues concerning experimental setup and technique must be addressed. First, the effect of splitter plates used to simulate planes of symmetry on the flowfield needs to be quantified to some degree. The leading edges of the splitter plates introduce shocks into the system that otherwise would not be present. This is clearly the case, as will be seen, where the splitter plates in the flush position cause a detached shock to form ahead of the sabot. Additionally, boundary layers form on the surface areas of the splitter plates, which affect the flowfield. This is most evident in the measured pressure increase at the tail of the sabot. The experimental data all show sharp pressure increases at the tail of the sabot. Although it is reasonable to expect that flow choking down through a reduced area would cause a pressure increase, it appears that the boundary layers from the splitter plates reduce the effective flow area so that a much higher pressure increase is seen than would otherwise occur.

Centerline Pressure Distribution

The centerline pressure distribution along the sabot was measured and compared to the results predicted by the AVCO code and by the analytical model for the four AOA studied. A photograph of the experimental model is shown without the splitter plates in Fig. 7a, and a schematic of the experimental model with the splitter plates is shown in Fig. 7b at 14-deg AOA. The results are presented in

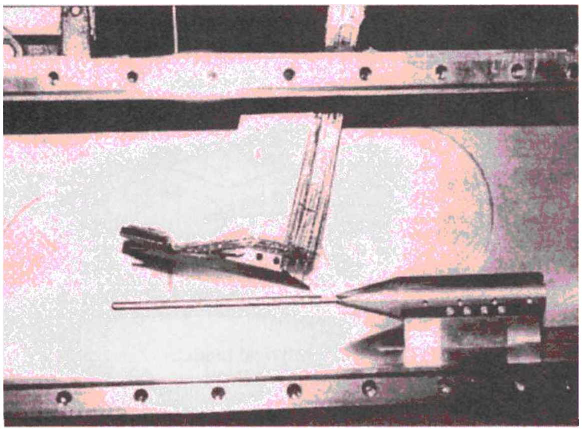

a) Without splitter plates

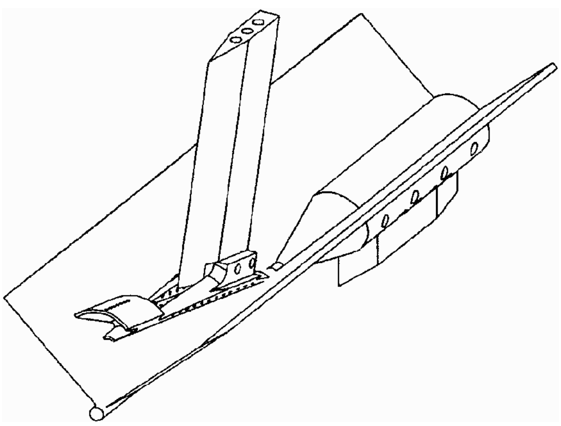

b) With splitter plates, 14-deg AOA

Fig. 7 Experimental model mounted in wind tunnel.

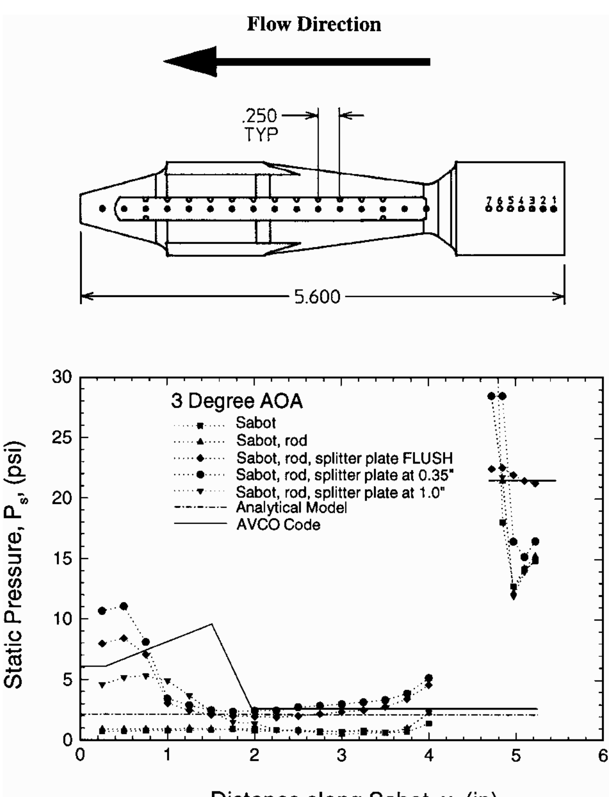

Fig. 8 Experimental and computed pressure distribution along centerline of sabot front scoop and underside, 3-deg AOA.

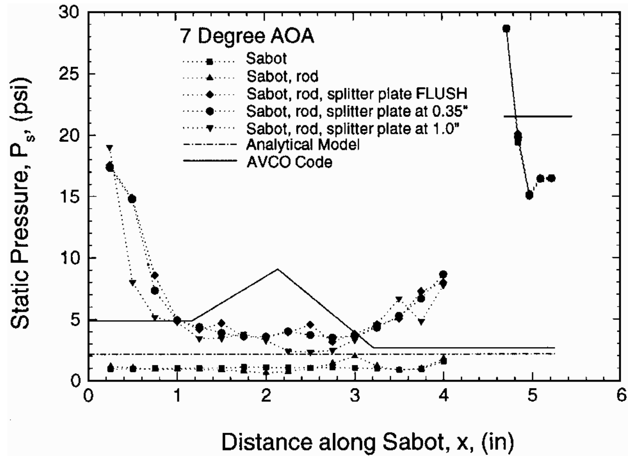

a) 7-deg AOA

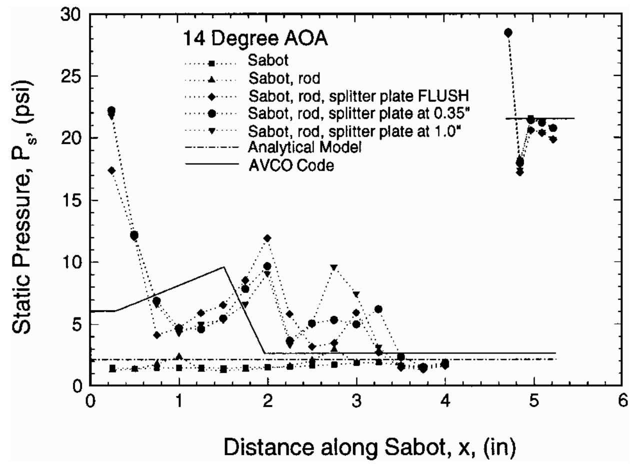

b) 14-deg AOA

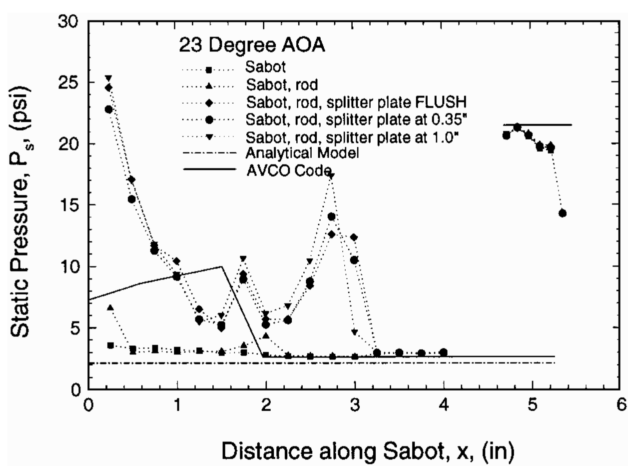

c) 23-deg AOA

Fig. 9 Experimental and computed pressure distribution along centerline of sabot front scoop and underside.

Fig. 8 for 3-deg AOA and in Figs. 9a–9c for 7, 14, and 23-deg AOA, respectively. Because the pressure distribution on the sabot is divided into two primary regions, i.e., front scoop and sabot underside, it is convenient to discuss these two regions separately, beginning with the sabot underside.

The 3-deg-AOA case is shown in Fig. 8. For reference, the sabot is shown with the locations of the pressure taps along the sabot underside. The distance on the underside of the sabot is measured from the sabot tail, and the flow direction is from right to left. The figure shows experimental data for sabot only, sabot and rod only, splitter plates flush with the tip of the rod, and splitter plates set back 0.35 in. and 1.0 in. from the tip of the rod. The figure also shows

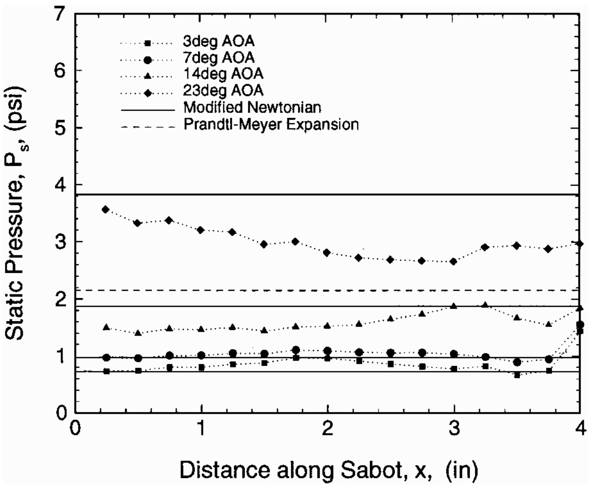

Fig. 10 Experimental and predicted centerline pressure distribution, sabot only, at 3-, 7-, 14-, and 23-deg AOA.

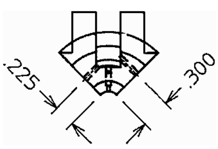

Fig. 11 Radial locations of pressure measurements on sabot side-face areas.

the pressure predicted by the analytical model and the AVCO code. The same data are shown in Fig. 9 for the other AOA.

Several observations can be made about all AOA. Concerning the centerline pressure distribution on the underside of the sabot, $0 \leq x \leq 4$, for the sabot and sabot-rod-only cases, the pressure distributions along the underside are very nearly constant and correspond closely to that predicted by the Prandtl–Meyer expansion modeled in the AVCO code and analytical model, and even more closely, as shown in the following section, to Newtonian pressure distribution. When splitter plates are present, the pressure distribution shows one or more sharp peaks, and in all cases shows a sharp increase in pressure at the tail of the sabot. It also is seen that the splitter plates tend to raise the base pressure above the value when no splitter plates are present. This is especially evident at the smaller AOA. The AVCO code adequately predicts the magnitude of the pressure peaks at nearly all AOA. However, it does not predict the double peak present in some cases, and in all cases misses the axial location of the pressure peak. The analytical model does not incorporate a pressure pulse model.

As stated earlier, the centerline pressure data appear to indicate that the modified Newtonian method may be a better approximation than the Prandtl–Meyer expansion model incorporated into the code. This is illustrated in Fig. 10, which shows the experimental centerline pressure distribution along with the predicted values computed using both methods. It is easily seen that the modified Newtonian method generally predicts the pressure level more accurately than the Prandtl–Meyer expansion method. It also displays the angle-of-attack sensitivity of the data, unlike the Prandtl–Meyer expansion technique, which is independent of AOA. Only the 23-deg-AOA

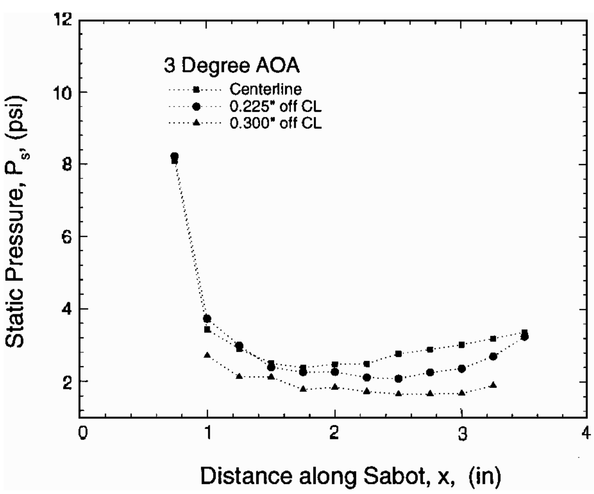

a) 3-deg AOA

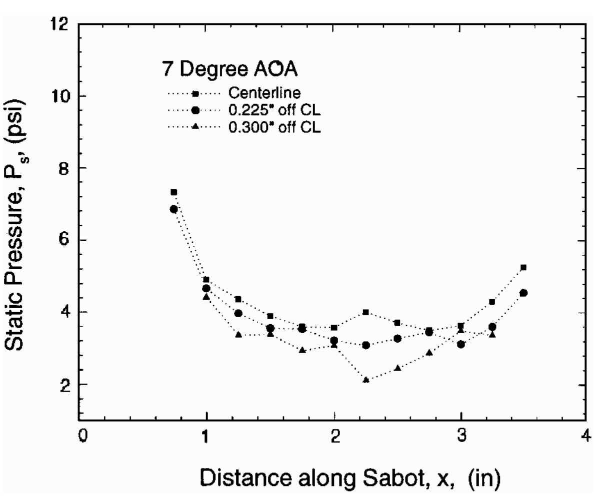

b) 7-deg AOA

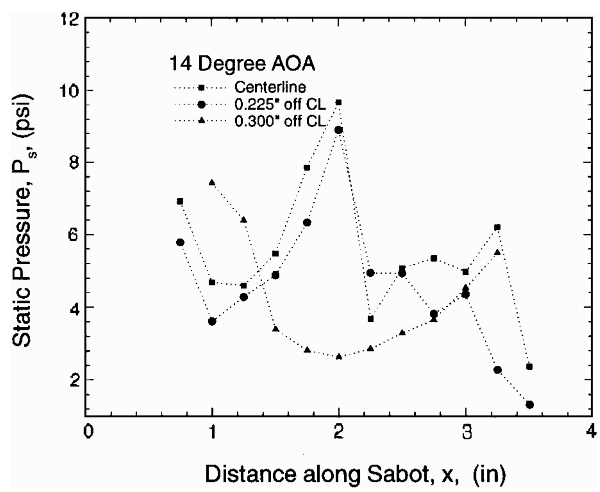

c) 14-deg AOA

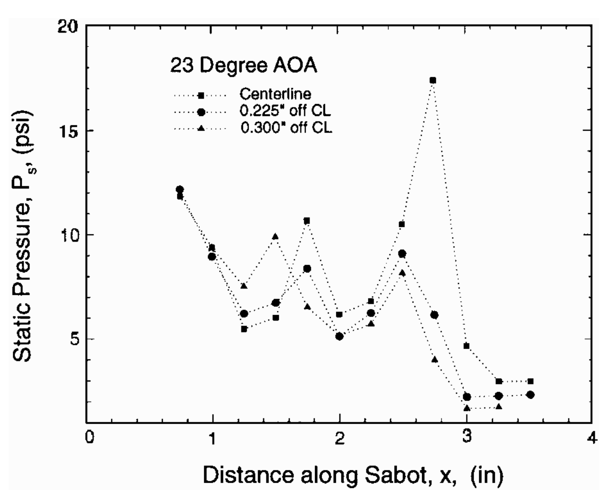

d) 23-deg AOA

Fig. 12 Pressure variation on sabot side-face area in radial direction.

prediction shows a large departure from the experimental data. It is unclear why this is so.

Front-Scoop Pressure Distribution

The pressure distributions on the front scoop of the sabot for each AOA also are shown in Figs. 8 and 9. The data indicate that the centerline pressure on the front scoop is sensitive to AOA. The front-scoop pressure model incorporated into the modified version of the AVCO code[7] assumes that the pressure on the front scoop is uniformly at the stagnation pressure corresponding to the freestream Mach number and does not include AOA dependence.

At 3-deg AOA, the data clearly show that the shock is not fully detached. Oblique shocks most likely form on the forward portions of the scoop, as indicated by the lower pressures, which reflect off the rear portion of the scoop, producing high pressures on that portion of the scoop. The only case not displaying this behavior is when the splitter plates are flush with the tip of the rod. In this case, the pressure on the front scoop is uniformly at the stagnation pressure corresponding to the freestream Mach number. It is obvious that the forward presence of the splitter plates causes a detached shock to form ahead of the sabot.

At 7-deg AOA it is clear that there is still an oblique shock structure on the forward portion of the front scoop. However, as the AOA increases to 14 deg and then 23 deg, the data indicate that the shock is becoming fully detached, and the pressures predicted by the AVCO code are beginning to agree with the experimental data. Note that these are all centerline data. There was not enough space in the front scoop to place pressure taps at other circumferential locations to investigate the pressure gradient in the circumferential direction. One would expect that as the flow is turned into the circumferential direction and begins to accelerate, pressures would decrease from centerline values. Because the net lifting force and pitching moment are computed from integrated values of the pressure distribution, a negative pressure gradient in the circumferential direction would tend to reduce the net lifting force and pitching moment.

Radial Pressure Variation

In addition to the centerline pressure distribution, pressure measurements were taken at the same axial locations on the sabot side-face areas, but at radial locations of 0.225 and 0.300 in. to determine whether significant pressure gradients exist on the side-face areas of the sabot in the radial direction. These locations are illustrated in Fig. 11. The results for the four AOA are shown in Figs. 12a–12d. The trends for each AOA are similar. As expected, there is a decrease in pressure in the radial direction, as the flow begins to accelerate around the sabot. In most cases the pressure change is small. However, at 14- and 23-deg AOA, the pressure pulse that appears at the centerline diminishes on the outer portion of the side-face area, indicating that the shock interaction is three dimensional and weaker as the flow moves away from the centerline. Previous comments about net lifting force and pitching moment apply here as well. If the pressure decreases significantly in the radial direction on the side-face area, this would tend to decrease the net lifting force and pitching moment.

Conclusions and Recommendations

Experimental and computational investigations of the pressure distribution on a sabot in hypervelocity flight were performed. The purpose was to determine whether the modifications made to the AVCO code accurately predict the pressure on the sabot front scoop and underside or whether further refinement to the aerodynamic model is indicated.

Comparing the data to the predicted results indicates that, although the model does a fair job of predicting the pressure distribution, further refinement to some portions of the model may be needed, especially the front scoop.

Even with the known limitations of the experimental setup, the following conclusions can be made.

1) The modified Newtonian method tends to predict the base pressure better than the Prandtl–Meyer expansion method.

2) The AVCO code predicts the pressure increase at the tail of the sabot well.

3) The AVCO code predicts the magnitude of the pressure pulse well but misses the axial location of the pulse.

4) The assumption of stagnation pressure on the entire face of the front scoop for all AOA does not accurately reflect the pressure distribution on the front scoop at all stages of the discard process.

5) The pressure pulse on the sabot underside tends to diminish on the outer portion of the side-face area and is not modeled with the current version of the AVCO code.

6) The analytical solution predicts the radial displacement very well for the cases considered here.

To improve the aerodynamic model in the AVCO code, several recommendations are made.

Use modified Newtonian pressure distribution to compute the base pressure on the underside of the sabot. The modified Newtonian method does a better job of predicting the base pressure and displays the AOA sensitivity of the experimental data.

Further investigate the pressure distribution on the front scoop. This requires a superscale model of the front scoop only, on which pressure taps could be placed at several circumferential locations to investigate the pressure variations in the circumferential direction.

Based on the results of the experimental investigation, modify the front-scoop aerodynamic model to more accurately represent the pressure on the front scoop at all stages of the discard process. This should include a pressure gradient in the circumferential direction if the experimental investigation shows it to be significant.

Perform the experiment using a four-petal sabot configuration so that any possible effect of splitter plates can be eliminated.

Acknowledgment

This work was supported by the U.S. Army Research Laboratory under Contract DAAA21-93-C-0101.

References

[1]Crimi, P., and Siegelman, D., "Analysis of Mechanical and Gasdynamic Loadings During Sabot Discard from Gun-Launched Projectiles," U.S. Army Ballistic Research Lab., Rept. BRL-CR 341, Aberdeen Proving Ground, MD, June 1977.

[2]Crimi, P., and Siegelman, D., "Projectile/Sabot Discard Aerodynamics," U.S. Army Ballistic Research Lab., Rept. BRL-CR-00410, Aberdeen Proving Ground, MD, Dec. 1979.

[3]Siegelman, D., and Wang, J., "Sabot Design Optimization," U.S. Army Ballistic Research Lab., Rept. ARBRL-CR-00450, Aberdeen Proving Ground, MD, March 1981.

[4]Siegelman, D., Wang, J., and Crimi, P., "Computation of Sabot Discard," U.S. Army Ballistic Research Lab., Rept. ARBRL-CR-00505, Aberdeen Proving Ground, MD, Feb. 1983.

[5]Sepri, P., "Aerodynamic Interaction Between Projectile Fins and Sabot Petals," Contract DAAG29-81-D0100, Sept. 1986.

[6]Savik, D., "AVCO Sabot Discard Program," U.S. Army Research Lab., ARL Internal Rept., Aberdeen Proving Ground, MD, 1986.

[7]Guillot, M., and Reinecke, W., "A Numerical and Experimental Investigation of Sabot Separation Dynamics," Inst. for Advanced Technology, IAT.R 0074, Austin, TX, Sept. 1995.

[8]Guillot, M., and Reinecke, W., "A Numerical and Experimental Investigation of Sabot Separation Dynamics," AIAA Paper 96-3100, Jan. 1996.

[9]Schmidt, E., "Wind Tunnel Measurements of Sabot Discard Aerodynamics," U.S. Army Ballistic Research Lab., ARBRL-TR-02246, Aberdeen Proving Ground, MD, July 1980.

[10]Dick, J. N., "Experimental Determination of Sabot Separation in a Mach 5 Wind Tunnel," M.S. Thesis, Univ. of Texas, Austin, TX, May 1996.

J. R. Maus
Associate Editor